Probabilistic Process-Structure-Property Modelling for Hardness and Porosity Estimation in High-Speed DED-Reprocessed Components in the context of the Circular Factory

Luisa Hoffmann[1], Mehdi Khabou[2], Helena Wexel[3], Ali Darijani[4], Jürgen Beyerer[4,5], Frederik Zanger[3], Volker Schulze[2,3], Stefan Dietrich[2], and Michael Heizmann[1]

[1] Institute of Industrial Information Technology (IIIT),
[2] Institute for Applied Materials – Materials Science and Engineering (IAM)
[3] Institute of Production Science (WBK)
[4] Vision and Fusion Laboratory (IES)
[5] Fraunhofer Institute of Optronics, System Technologies and Image Exploitation (IOSB)
luisa.hoffmann@kit.edu

Abstract. In Circular Factory (CF) environments, used components are disassembled, characterized, and reprocessed, based on a reliable estimation of the resulting material properties and taking measurement and remanufacturing uncertainties into consideration. For reprocessing steps such as High-Speed Laser Directed Energy Deposition (HS DED-LB), uncertainties and process variability critically affect the robustness and stability of process-structure-property predictions. Additionally, measurements introduce uncertainties that propagate into the estimation of the post-process material state. For remanufactured structural components, hardness and porosity serve as key quality indicators describing the material state. Both are investigated as key determinants of fatigue performance, since hardness governs local fatigue strength, while porosity acts as a stress concentrator that promotes early fatigue crack initiation and reduces fatigue strength and component lifetime. In HS DED-LB, laser power and scan speed govern the thermal input and thereby influence microstructure development and resulting material properties. The process parameters can act as physically based features representing the thermal history and its fluctuations to correlate the process to the material state. To address this issue, Gaussian Mixture Models (GMMs) are adopted as a unified probabilistic framework to represent multimodal uncertainty and enable consistent inference under process variability and measurement noise. This paper presents a probabilistic approach for modelling and fusing measurement and process uncertainties using GMMs, resulting in probability density functions of hardness and porosity after HS DED-LB reprocessing. The approach enables uncertainty-aware estimation of the material state and supports adaptive tuning of reprocessing parameters to achieve the desired target quality characteristics in circular factories.

Keywords: Circular Factory · Uncertainty quantification · Gaussian mixture.

1 Introduction

The transition from linear manufacturing toward sustainable and resource-efficient production systems has increased interest in Circular Factory (CF) concepts. In such environments, used components are inspected, characterized, and reprocessed to extend their service life and reduce material consumption [1]. Since reprocessing decisions are often made for individual components with uncertain material states and process conditions, reliable uncertainty-aware estimation is essential for quality assessment and process control.

Process-structure-property (PSP) modelling provides a means to relate manufacturing conditions to resulting material properties and has become an important approach in additive manufacturing [2]. Data-driven approaches, including regression and surrogate models, have been developed to learn these relationships from experimental and simulated data [2, 3]. Probabilistic approaches, such as Gaussian-process-based surrogate models, additionally enable uncertainty quantification [3]. However, these approaches typically formulate PSP modelling as a regression problem rather than representing the joint probability distribution of process variables, observations, and material properties.

This is particularly relevant for remanufacturing processes, where both process conditions and measurements are uncertain. High-Speed Laser Directed Energy Deposition (HS DED-LB) enables the localized restoration of worn or damaged components, but the resulting material properties depend strongly on the thermal history governed by process parameters such as laser power and scan speed. Pyrometric monitoring provides high-temporal-resolution temperature measurements; however, spatter, smoke, plasma formation, and variations in surface emissivity introduce measurement uncertainty [4]. Treating the measured temperature as an exact process variable may therefore lead to overconfident material-property predictions.

This work proposes a probabilistic PSP framework based on Gaussian Mixture Models (GMMs) for uncertainty-aware modelling of HS DED-LB reprocessing in Circular Factory environments. Process parameters, pyrometric measurements, hardness, and porosity are represented jointly within a unified probabilistic model. Uncertain temperature observations are incorporated as soft evidence, and analytical conditioning of the joint GMM yields probability density functions of the resulting material properties. The proposed framework thereby enables explicit propagation of process and measurement uncertainty for probabilistic quality assessment and reprocessing decisions.

2 Experimental Setup and Data Acquisition

2.1 High-Speed Directed Energy Deposition Process

The experimental investigations were conducted using a High-Speed Laser Directed Energy Deposition (HS DED-LB) process for reprocessing metallic components. In this process, AISI 4140 powder, corresponding to 42CrMo4 [5], was locally melted by the laser beam and was deposited onto the surface of the component to be reprocessed. The material was applied track-wise and layer-wise onto the substrate while the thermal behavior of the melt pool region was monitored continuously [6].

The primary process parameters considered in this work are the laser power P and the process speed v. Both parameters control the linear energy input into the material and therefore strongly affect melt pool formation, thermal history, microstructure evolution, and resulting material properties [7]. To investigate the relationship between process parameters and the resulting material state, multiple samples were manufactured using different parameter combinations. The ratio P/v was additionally considered as a simplified proxy for the line energy input. This descriptor does not represent the full effective heat input, since absorptivity, powder feed rate, laser spot size, layer geometry, and heat dissipation are not explicitly included. Process parameters were varied within a nested design comprising a full-factorial core ($P = 2350 - 2650W$, $v = 40 - 60mm/s$, 25 combinations) supplemented by extended validation points at the boundaries of the process window ($P = 2200 - 2800W$), resulting in 41 manufactured specimens in total. Of these, 17 specimens spanning the full range of P/v ratios were selected for detailed material characterization. The other experimental setup parameters are listed in Table 1.

Table 1. Process parameters for the powder delivery and shielding system

Parameter	Value
Working distance	Powder focus position +1 mm
Laser beam diameter	1 mm
Rotational speed of powder feeder	5 rpm
Powder mass flow rate	15.125 g/min
Carrier gas flow rate	8 l/min
Shielding gas flow rate	20 l/min

Temperature measurements were acquired during the process using a pyrometric monitoring system. Pyrometers provide high temporal resolution and enable non-contact observation of the thermal process zone. However, the acquired signals are affected by stochastic variability and systematic disturbances caused by process-related phenomena such as spatter formation, smoke, plasma interactions, and changing surface emissivity [4]. These effects introduce fluctuations and potential bias into the recorded pyrometric temperature signal [8].

Furthermore, the measurement system records data continuously during the entire manufacturing process, including machine movements outside the actual deposition region. Consequently, the raw temperature data also contain measurements that are not directly associated with material deposition. To obtain representative process information, the data were filtered to retain deposition-related process phases. Figure 1 illustrates the temporal evolution of the measured temperature signal and the filtered deposition-related observations.

The resulting filtered temperature distributions exhibit characteristic variations associated with different thermal process states. The right plot in Figure 1 shows the histogram of the filtered temperature measurements for a representative sample. These distributions contain information on process variability and pyrometric measurement uncertainty and are therefore used as probabilistic process descriptors in the subsequent modelling framework.

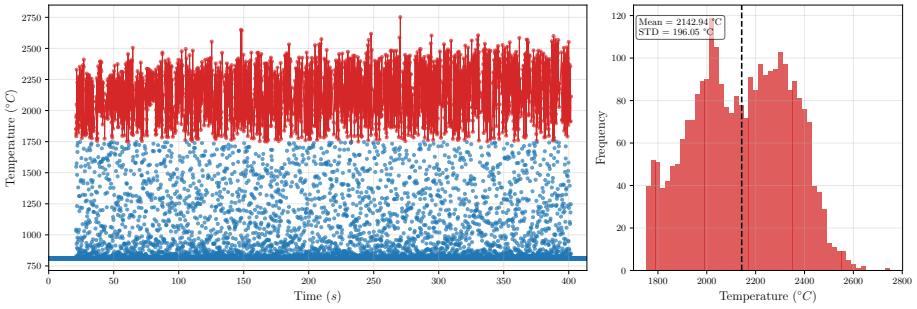


Fig. 1. Left: Temperature data over time during the process with process parameters $v = 45\,\mathrm{mm/s}$ and $P = 2575\,\mathrm{W}$. The blue data is filtered, and the red data is used for further processing. Right: Histrogram of the filtered temperature data

2.2 Material Characterization

After the remanufacturing process, the resulting material state was characterized by hardness and porosity measurements. Hardness was measured using a Qness microindentation system (Vickers microhardness). To account for spatial material inhomogeneity introduced by the additive manufacturing process, hardness measurements were performed at different depths within the deposited material, along the build direction. Since the deposited layers experience different thermal histories, the hardness is not expected to be homogeneous across the build height. Multiple hardness measurements were therefore conducted for each sample to obtain representative mean values and standard deviations. The observed hardness scatter may result through local microstructural variations [9], porosity, heat accumulation, and spatially varying heat dissipation conditions within the deposited material.

Porosity was quantified by two-dimensional image analysis of metallographically prepared cross-sections acquired with an optical microscope. Porosity characterization was performed to quantify process-induced defects within the deposited material. The observed porosity values exhibit statistical variability due to the stochastic nature of defect formation during the HS DED-LB process. Typical pore formation mechanisms include gas entrapment, lack of fusion, and keyhole-induced porosity. These mechanisms are strongly affected by the selected process parameters and local boundary conditions, such as thermal history, melt pool stability, powder delivery, and heat dissipation [10].

Both properties are relevant quality indicators for remanufactured structural components, as they strongly affect fatigue performance and component lifetime [1]. The experimentally obtained process parameters, pyrometric temperature measurements, hardness values, and porosity measurements form the basis for the probabilistic process-structure-property modelling approach proposed in this work.

3 Methodology

3.1 Gaussian Mixture

Gaussian Mixture Models (GMMs) are a powerful tool that enable many calculations to be performed in closed form. Thanks to their parametric representation, complex distributions can be described concisely by specifying the mixture parameters [11]. Using the measurement data, which includes the uncertainty in temperature, hardness, and porosity, we fit a joint GMM. The motivation for using a GMM is that the observed data are generated by multiple underlying stochastic processes and are subject to measurement noise and epistemic uncertainty. A single Gaussian distribution is therefore often insufficient to capture the full structure of the data, whereas a mixture of Gaussians can approximate complex, multimodal distributions. Let $\mathbf{x} \in \mathbb{R}^d$ denote a random vector representing the measured variables (temperature, process parameters, hardness, and porosity). A Gaussian mixture model defines the probability density function as

$$p(\mathbf{x}) = \sum_{k=1}^{K} \pi_k \mathcal{N}(\mathbf{x} \mid \boldsymbol{\mu}_k, \boldsymbol{\Sigma}_k), \tag{1}$$

where K is the number of mixture components, π_k are the mixing coefficients satisfying $\pi_k \geq 0$ and $\sum_{k=1}^{K} \pi_k = 1$, and $\mathcal{N}(\mathbf{x} \mid \boldsymbol{\mu}_k, \boldsymbol{\Sigma}_k)$ denotes the multivariate Gaussian distribution with mean vector $\boldsymbol{\mu}_k$ and covariance matrix $\boldsymbol{\Sigma}_k$. The model parameters $\{\pi_k, \boldsymbol{\mu}_k, \boldsymbol{\Sigma}_k\}_{k=1}^{K}$ were estimated from the measurement data using the Expectation–Maximization (EM) algorithm [12]. In the expectation step, posterior probabilities for the assignment of each observation to the individual mixture components are computed. In the maximization step, the model parameters are updated by maximizing the expected log-likelihood of the data. These two steps are iteratively repeated until convergence of the likelihood

function is achieved. The optimal number of mixture components K was determined using information-theoretic model selection criteria such as the Bayesian Information Criterion (BIC) and the Akaike Information Criterion (AIC). These criteria balance model complexity and goodness of fit, thereby preventing overfitting while ensuring an adequate representation of the underlying data distribution. In this framework, each mixture component can be interpreted as representing a latent regime of the measurement process, capturing different sources of uncertainty in process parameters, temperature, hardness, and porosity. The fitted GMM therefore provides a flexible probabilistic representation of the joint data distribution. The resulting joint distribution of hardness and porosity is illustrated in Fig. 2 as a GMM, where each component is visualized as a 3-dimensional covariance ellipsoid at two standard deviations. The figure demonstrates how the learned mixture model captures multimodal dependencies and correlations between the material properties.

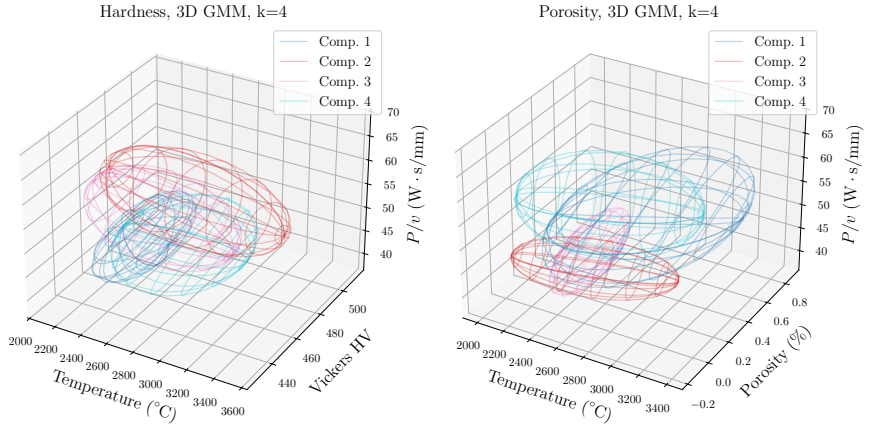


Fig. 2. Joint GMM for hardness (left) and porosity (right) with 4 mixture components each, where each component is visualized as a 3-dimensional covariance ellipsoid at two standard deviations

The probabilistic framework therefore enables both uncertainty quantification and data-driven inference of material properties from partially observed measurements.

3.2 Conditioning

Once trained on the experimental data, the model can be conditioned on observed variables in order to infer instance-specific probabilistic predictions for

unknown quantities. Here, the subscript t refers to target variables (quantities to be inferred), while o denotes observed variables (conditioning evidence).

In practical settings, observations are uncertain and represented as a GMM:

$$q(\mathbf{x}_o) = \sum_{m=1}^{M} w_m \mathcal{N}(\mathbf{x}_o \mid \boldsymbol{\nu}_m, \mathbf{R}_m), \tag{2}$$

where $\boldsymbol{\nu}_m$ and $\mathbf{R}_m$ denote the mean and covariance of the m-th observation component, and w_m are the associated mixture weights satisfying $\sum_{m=1}^{M} w_m = 1$, $w_m >= 0$.

The joint covariance of each mixture component is partitioned as

$$\boldsymbol{\Sigma}_k = \begin{pmatrix} \boldsymbol{\Sigma}_{tt,k} & \boldsymbol{\Sigma}_{to,k} \\ \boldsymbol{\Sigma}_{ot,k} & \boldsymbol{\Sigma}_{oo,k} \end{pmatrix}. \tag{3}$$

Conditioning the joint GMM on this soft evidence yields a posterior distribution that is itself a GMM:

$$p(\mathbf{x}_t \mid E) = \sum_{k=1}^{K} \sum_{m=1}^{M} \alpha_{k,m} \, \mathcal{N}(\mathbf{x}_t \mid \boldsymbol{\mu}_{k,m}^{+}, \boldsymbol{\Sigma}_{k,m}^{+}). \tag{4}$$

For each pair (k, m):

$$\mathbf{S}_{k,m} = \boldsymbol{\Sigma}_{oo,k} + \mathbf{R}_m, \tag{5}$$

$$\boldsymbol{\mu}_{k,m}^{+} = \boldsymbol{\mu}_{t,k} + \boldsymbol{\Sigma}_{to,k} \mathbf{S}_{k,m}^{-1} (\boldsymbol{\nu}_m - \boldsymbol{\mu}_{o,k}), \tag{6}$$

$$\boldsymbol{\Sigma}_{k,m}^{+} = \boldsymbol{\Sigma}_{tt,k} - \boldsymbol{\Sigma}_{to,k} \mathbf{S}_{k,m}^{-1} \boldsymbol{\Sigma}_{ot,k}. \tag{7}$$

Weights are given by

$$\tilde{\alpha}_{k,m} = \pi_k w_m \, \mathcal{N}(\boldsymbol{\nu}_m \mid \boldsymbol{\mu}_{o,k}, \mathbf{S}_{k,m}), \tag{8}$$

with normalization

$$\alpha_{k,m} = \frac{\tilde{\alpha}_{k,m}}{\sum_{k,m} \tilde{\alpha}_{k,m}}. \tag{9}$$

These formulas are known as conditional Gaussian distributions [13] [14]. This formulation can be interpreted as a probabilistic generalization of classical conditioning. Instead of conditioning on a single deterministic measurement, the inference process incorporates an entire uncertainty distribution over the observed variables. Consequently, uncertainty in the measurements propagates consistently through the joint GMM and is reflected in the posterior distribution of the target variables.

The classical conditioning formulas are recovered as a limiting case when the observation uncertainty vanishes, i.e., $\mathbf{R}_m \to \mathbf{0}$. In this case, the soft evidence reduces to a deterministic observation, and the formulation becomes equivalent to conditioning with hard evidence. This conditioning procedure enables the generation of instance-specific probabilistic predictions. For example, given observed process parameters and temperature values, the conditioned GMM can infer the corresponding probability distributions of hardness and porosity.

4 Results and Discussion

The fitted GMM provides a probabilistic representation of the experimentally observed process and material-property distributions. To assess whether the model adequately represents the experimental data, the marginal distributions obtained from the joint GMM are compared with the corresponding measured distributions. The proposed probabilistic PSP framework based on GMMs enables a joint representation of process parameters, thermal measurements, and resulting material properties, namely hardness and porosity (see Fig. 2). In contrast to deterministic approaches, the model does not provide single-point estimates but yields full probability density functions (PDFs) for hardness and porosity conditioned on observed process states. For the investigated process condition, the predicted hardness distribution is concentrated around $469.45HV$, whereas the predicted porosity distribution exhibits bimodal behavior. The different distribution widths indicate that the two quality indicators are affected differently by the uncertainty in the observed process state.

Conditioning the model on observed process parameters and temperature measurements, which are assumed to follow a Gaussian distribution with a mean and a standard deviation (see histogram in Fig. 1) in this case, results in instance-specific posterior distributions of hardness and porosity, as shown in Fig. 3. The width of these distributions directly reflects the propagated uncertainty from both process variability and sensor noise. Higher uncertainty in temperature measurements leads to broader posterior distributions, indicating reduced confidence in the inferred material state.

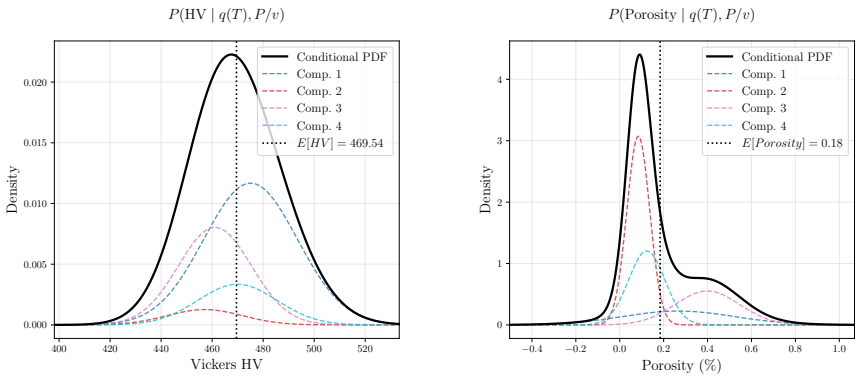


Fig. 3. Resulting PDF for hardness and porosity for a given Temperature $q(T) = \mathcal{N}(T \mid 2200°\text{C}, 220°C)$ and given process parameters $P/v = 51\text{W} \cdot \text{s/mm}$

The probabilistic nature of the GMM further reveals multimodal behavior in the data. These modes can be interpreted as latent process regimes induced

by variations in thermal input during HS DED-LB processing. In particular, fluctuations in laser power and scan speed lead to distinct thermal histories, which are reflected in different clusters of the learned distribution.

From a process control perspective, the resulting PDFs provide significantly richer information than deterministic predictions. Instead of a single estimated hardness or porosity value, the framework enables the evaluation of confidence intervals and risk-aware decision making. For example, components with high predicted variance in hardness can be flagged for additional inspection or reprocessing within a circular manufacturing workflow. Overall, the results demonstrate that the proposed GMM-based PSP framework is capable of capturing nonlinear dependencies, multimodality, and uncertainty propagation in HS DED-LB reprocessing data. This makes it particularly suitable for remanufacturing scenarios where both process variability and measurement uncertainty are inherent.

5 Conclusion

This work presented a probabilistic process-structure-property modelling framework for hardness and porosity estimation in High-Speed Laser Directed Energy Deposition (HS DED-LB) reprocessed components within circular factory environments. The proposed approach integrates process parameters, pyrometric temperature measurements, and material characterization data into a joint Gaussian Mixture Model. By explicitly modelling measurement uncertainty and process variability, the framework enables uncertainty-aware inference of material properties. Through conditional probabilistic reasoning, instance-specific probability density functions for hardness and porosity can be derived from partially observed process data.

The results demonstrate that additive manufacturing data exhibits multimodal and stochastic characteristics that cannot be adequately captured using deterministic models. In contrast, the proposed GMM formulation provides a flexible representation of latent process regimes and enables consistent uncertainty propagation from process monitoring to material property estimation.

From an application perspective, the probabilistic output of the model supports decision-making in circular manufacturing systems by enabling risk-aware quality assessment and adaptive process control [15]. Future work will focus on incorporating spatially resolved microstructural descriptors and extending the framework toward physics-informed probabilistic models. In addition, real-time inference strategies for in-situ process control will be investigated to enable closed-loop optimization of HS DED-LB parameters in circular production environments.

Acknowledgment

This research is funded by the Deutsche Forschungsgemeinschaft (DFG, German Research Foundation) in the collaborative research center (CRC) 1574 “Circular Factory for the Perpetual Product” with the project ID 471687386.

References

1. I. Gibson, D. Rosen, B. Stucker, and M. Khorasani, *Additive Manufacturing Technologies*. Switzerland: Springer Nature Switzerland, 3 ed., 2021.
2. Z. Wang, W. Yang, Q. Liu, Y. Zhao, P. Liu, D. Wu, M. Banu, and L. Chen, "Data-driven modeling of process, structure and property in additive manufacturing: A review and future directions," *Journal of Manufacturing Processes*, vol. 77, pp. 13–31, 2022.
3. R. N. Saunders, K. Teferra, A. Elwany, J. G. Michopoulos, and D. Lagoudas, "Metal am process-structure-property relational linkages using gaussian process surrogates," *Additive Manufacturing*, vol. 62, p. 103398, 2023.
4. E. Popova, T. M. Rodgers, X. Gong, A. Cecen, J. D. Madison, and S. R. Kalidindi, "Process-structure linkages using a data science approach: Application to simulated additive manufacturing data," *Integrating Materials and Manufacturing Innovation*, vol. 6, no. 1, pp. 54–68, 2017.
5. J. Damon, R. Koch, D. Kaiser, G. Graf, S. Dietrich, and V. Schulze, "Process development and impact of intrinsic heat treatment on the mechanical performance of selective laser melted AISI 4140," *Additive Manufacturing*, vol. 28, pp. 275–284, Aug. 2019.
6. H. Wexel, P. Fischmann, J. Schubert, and F. Zanger, "High-speed ded-lb: Analysis of process control variables as enabler for remanufacturing of unique products," *Procedia CIRP*, vol. 127, pp. 230–235, 2024. 10th CIRP Conference on Assembly Technology and Systems (CIRP CATS 2024).
7. W. E. King, H. D. Barth, V. M. Castillo, G. F. Gallegos, J. W. Gibbs, D. E. Hahn, C. Kamath, and A. M. Rubenchik, "Observation of keyhole-mode laser melting in laser powder-bed fusion additive manufacturing," *Journal of Materials Processing Technology*, vol. 214, no. 12, pp. 2915–2925, 2014.
8. S. Maffia, V. Furlan, and B. Previtali, "Molten pool temperature monitoring in laser metal deposition: Comparison between single wavelength and ratio pyrometry techniques," *International Journal of Mechatronics and Manufacturing Systems*, vol. 16, no. 1, pp. 96–111, 2023.
9. S. Cooke, G. Sweet, K. Ahmadi, P. Bishop, and R. Herring, "Thermo-mechanical-metallurgical modelling, validation and characterization of 42CrMo4 steel processed by directed energy deposition," *Journal of Manufacturing Processes*, vol. 81, pp. 537–561, Sept. 2022.
10. A. Salmi, G. Piscopo, A. N. Pilagatti, and E. Atzeni, "Evaluation of Porosity in AISI 316L Samples Processed by Laser Powder Directed Energy Deposition," *Journal of Manufacturing and Materials Processing*, vol. 8, p. 129, June 2024.
11. A. Darijani, J. Beyerer, Z. S. H. Nasrollah, L. Hoffmann, and M. Heizmann, "Comprehensive description of uncertainty in measurement for representation and propagation with scalable precision," 2026. arXiv preprint arXiv:2603.20365.
12. A. P. Dempster, N. M. Laird, and D. B. Rubin, "Maximum likelihood from incomplete data via the em algorithm," *Journal of the Royal Statistical Society. Series B (Methodological)*, vol. 39, no. 1, pp. 1–38, 1977.
13. K. P. Murphy, *Probabilistic Machine Learning: An introduction*. MIT Press, 2022.
14. C. M. Bishop, *Pattern Recognition and Machine Learning (Information Science and Statistics)*. Berlin, Heidelberg: Springer-Verlag, 2006.
15. N. Afifi, V. L. Mas, J. Hemmerich, F. Leitenberger, L. Hoffmann, A. Darijani, P. Grauberger, M. Heizmann, J. Beyerer, and S. Matthiesen, "Data-driven decision-making: Leveraging digital twins for reprocessing in the circular factory," *Zeitschrift für wirtschaftlichen Fabrikbetrieb*, vol. 120, no. s1, p. 170–176, 2025.